Available online at www.sciencedirect.com
ScienceDirect
Physics Letters A 372 (2008) 327–332
PHYSICS LETTERS A
www.elsevier.com/locate/pla

Interactions of solitons with complex defects in Bragg gratings

Peter Y.P. Chen [a,*], Boris A. Malomed [b], Pak L. Chu [c]

[a] *School of Mechanical and Manufacturing Engineering, University of New South Wales, Sydney 2052, Australia*
[b] *Department of Interdisciplinary Studies, School of Electrical Engineering, Faculty of Engineering, Tel Aviv University, Tel Aviv 69979, Israel*
[c] *Cotco Holdings Limited, Photonics Centre, Hong Kong Science Park, Hong Kong*

Received 14 March 2007; accepted 23 March 2007

Available online 28 March 2007

Communicated by V.M. Agranovich

Abstract

We examine collisions of moving solitons in a fiber Bragg grating with a *triplet* composed of two closely set repulsive defects of the grating and an attractive one inserted between them. A *doublet* (dipole), consisting of attractive and repulsive defects with a small distance between them, is considered too. Systematic simulations demonstrate that the triplet provides for superior results, as concerns the capture of a free pulse and creation of a *standing optical soliton*, in comparison with recently studied traps formed by single and paired defects, as well as the doublet: 2/3 of the energy of the incident soliton can be captured when its velocity attains half the light speed in the fiber (the case most relevant to the experiment), and the captured soliton quickly relaxes to a stationary state. A subsequent collision between another free soliton and the pinned one is examined too, demonstrating that the impinging soliton always bounces back, while the pinned one either remains in the same state, or is kicked out forward, depending on the collision velocity and phase shift between the solitons.

PACS: 42.65.Tg; 05.45.Yv; 42.79.Dj

1. Introduction

It is well known that the interplay of the linear transmission spectrum of a fiber Bragg gratings (FBG), which includes the bandgap, and material Kerr nonlinearity gives rise to robust optical pulses, which are often called gap solitons, or, more generally, Bragg-grating solitons. The solitons in FBGs were first predicted theoretically [1] (see also review [2]), and then created in the experiment [3]; later, solitons where also created in a photonic grating, induced in an ordinary fiber as a superposition of two mutually coherent pump beams [4]. The stability of solitons in the standard FBG model was investigated in detail by means of approximate semi-analytical [5] and accurate numerical [6] methods.

A well-known feature of the FBG model is that the soliton may have zero velocity, which suggests that fiber gratings may be appropriate media for the creation of stable pulses of *slow/standing light*, which is a problem of current interest [7], including the quest of slow optical solitons [8]. In the first experiments in the FBG, the smallest velocity of the soliton was $\simeq 0.5c_0$, with c_0 the speed of light in the fiber. Recently, an essentially new experimental result has been reported [9], with the soliton's velocity reduced to $0.16c_0$, which, quite feasibly, can be made still smaller by means of the technique applied in Ref. [9], viz., the use of an *apodized* FBG, with the grating strength gradually increasing along the fiber (theoretically, the use of an apodized FBG for the retardation of solitons and, eventually, bringing them to a halt was elaborated in detail in Ref. [10]).

Collisions of moving FBG solitons with local defects of the grating has also been the subject of several theoretical works [11–15]. A general objective of these studies was to predict a possibility of trapping a moving (relatively fast) soliton by a defect, and thus

* Corresponding author.
E-mail address: peterc@cdf.mech.unsw.edu.au (P.Y.P. Chen).

0375-9601/$ – see front matter
doi:10.1016/j.physleta.2007.03.060

transforming it into a stable *pinned optical soliton* [11,12]. Such an outcome may be of considerable interest, as, besides being a challenging problem to fundamental nonlinear optics and nonlinear-wave dynamics in general, it may find applications to the design of all-optical memory and logic elements, the trapped soliton playing the role of a data bit. In addition, the theoretical analysis has demonstrated that the attenuation of the pinned soliton due to the loss in the FBG material may be compensated by a localized gain, applied at the same position where the pinning defect was created [13]. Besides the soliton proper, one can also consider the interaction of a more general localized wave packet with FBG defects [14]. Similar interaction were examined in models of photonic crystals, which combine a Bragg grating and layers of resonantly absorbing atoms (see a review of the topic in Ref. [16]); in that case, a soliton may interact with an intrinsic defect of the photonic crystal [17].

An attractive local defect in the FBG may be realized as a local suppression of the grating. A repulsive defect is possible too, in the form of a short segment with enhanced Bragg reflectivity. In Refs. [11,12], it was concluded that three different outcomes of the collision of a free soliton with an attractive defect are possible, viz., transmission (i.e., passage of the soliton through the defect), capture, and splitting of the incident soliton into three pulses—transmitted, trapped, and reflected ones. Besides that, in the case when the incident soliton is "heavy" (i.e. intrinsically unstable [5,6]), almost all the energy may go into the reflected pulse, making the attractive defect to look as a repulsive one [12].

As concerns the primary goal, i.e., efficient capture of a relatively fast free soliton, it was demonstrated in Ref. [15] that better results might be provided not by a simple attractive defect, but rather by structures built as pairs of attractive defects separated by some distance, or, still more efficiently, by *cavities*, in the form of a pair repulsive local defects. While a single repulsive inhomogeneity cannot trap anything, the cavity has a strong potential for that (the trapped soliton then performs shuttle oscillations in the cavity). It was demonstrated that the paired defects, unlike the single attractive one, give rise to a well-defined region in the respective parameter space where the capture of the fast soliton is especially efficacious (up to velocities of the incident solitons $\simeq 0.35c_0$ and $\simeq 0.45c_0$, in the cases of the attractive and repulsive pairs, respectively).

The subject of the present work is to extend the analysis to collisions of solitons in the FBG with more complex (but still compact and quite simple, as concerns the fabrication) defects, built as a *doublet* (alias "dipole") and, chiefly, *triplet*, i.e., respectively, a pair of attractive and repulsive defects with a relatively small distance between them, or two repulsive defects with an attractive one placed between them. We conclude that the triplet is *superior* to all other trapping configurations: it provides for the capture of $2/3$ of the energy of the incident soliton at velocities attaining $0.5c_0$, and, which is quite important too, the trapped soliton quickly relaxes into a stationary state. The "quality" of the trapped soliton is attested to by its collision with a fresh soliton impinging upon the trapped one: while in other settings (including the newly introduced doublet) the outcome of the collision is actually unpredictable, as it strongly depends on the intrinsic state of the trapped soliton, that changes in time, for the soliton trapped by the triplet the outcome is reproducible. The fresh soliton always bounces back, while the pinned one either gets released, or remains pinned. These results may be useful in terms of the above-mentioned soliton-based memory and logic elements.

2. The model

Following Refs. [11,12] and [15], the FBG model with imperfections is based on the normalized coupled-mode equations for amplitudes of the right- and left-traveling electromagnetic waves, u and v:

$$\mathrm{i}\frac{\partial u}{\partial t}+\mathrm{i}\frac{\partial u}{\partial x}+v+\left(|u|^2/2+|v|^2\right)u=\kappa f(x)v, \tag{1}$$

$$\mathrm{i}\frac{\partial v}{\partial t}-\mathrm{i}\frac{\partial v}{\partial x}+u+\left(|v|^2/2+|u|^2\right)v=\kappa f(x)u, \tag{2}$$

where x and t are the coordinate along the fiber and time. The cross-phase-modulation coefficient, group velocity of the carrier waves, and Bragg reflectivity in the uniform grating are scaled to be 1. Function $f(x)$ in these equations describes the defect of the grating, with strength κ. Each individual defect is realized as a rectangular configuration, with $f(x)=1/\Delta x$ within a segment of length $\Delta x=0.469$, and $f(x)=0$ elsewhere, $\kappa>0$ and $\kappa<0$ corresponding to the attractive and repulsive defects, respectively. The rectangular shape of the defect approximates the δ-function profile assumed in previous studies [11,12,15]. In physical units, $\Delta x=1$ typically corresponds to length ~ 1 mm [2], while the actual size of the solitons created in the experiment may be $\lesssim 1$ cm [3,9], hence this approximation of $\delta(x)$ seems reasonable.

In this work, we deal with $f(x)$ corresponding to a dipole (doublet) set, composed of attractive and repulsive rectangular defects with a small distance between their edges, $\Delta x/4=0.117$, and (chiefly) a triplet set, consisting of two repulsive defects with an attractive one between them, with the same separation between adjacent defects (it was checked that, for the doublet and triplet alike, this small separation provides for optimum results, as concerns the capture of fast solitons).

The attractive defect is realized as a narrow segment of the FBG with suppressed grating. Therefore, as the full local reflectivity in Eqs. (1) and (2) cannot be negative, only $\kappa f(x)\leqslant 1$, i.e., values $\kappa\leqslant\Delta x\equiv 0.469$, are meaningful. Unlike that, $\kappa<0$, which corresponds to a local enhancement of the grating, is not subject to a specific limitation on $|\kappa|$ [15] (however, the form of the coupled-mode equations for a strong grating may alter [18]).

Solitons moving at velocity c (with $|c| < 1$) in the uniform FBG are given by the well-known solutions to Eqs. (1) and (2) with $\kappa = 0$ [1]:

$$\{u, v\}_{\rm sol} = \pm e^{i\Phi}\sqrt{\frac{2(1 \pm c)}{3 - c^2}}\left(1 - c^2\right)^{1/4}\{W, W^*\},$$
$$W(X) = \frac{\sin\theta}{\cosh(X\sin\theta - i\theta/2)},$$
$$\Phi = \frac{4c}{3 - c^2}\tan^{-1}\left[\tanh(X\sin\theta)\tan\frac{\theta}{2}\right] - T\cos\theta, \tag{3}$$

where $X \equiv (x - ct)/\sqrt{1 - c^2}$, $T \equiv (t - cx)/\sqrt{1 - c^2}$, and the soliton's amplitude, θ, takes values $0 < \theta < \pi$. Soliton family (3) is stable for $\theta \leqslant \theta_{\rm cr}(c)$, where $\theta_{\rm cr}(c = 0) \approx 1.01(\pi/2)$ [5,6], and $\theta_{\rm cr}$ very weakly depends on c, up to $c = 1$ [6]. We will consider solitons with $c < 0$; accordingly, the dipole set is built as a right attractive defect followed by a left repulsive one.

An exact solution is also available for a quiescent soliton pinned by the defect with $f(x) = \delta(x)$ [12],

$$\{u, v\} = \pm\sqrt{\frac{2}{3}}\,e^{-it\cos\theta}\frac{\sin\theta}{\cosh[(x + a\,\mathrm{sgn}\,x)\sin\theta \mp i\theta/2]}, \tag{4}$$

with $\tanh(a\sin\theta) = \tanh(\kappa/2)\cot(\theta/2)$. This solution exists for $2\tan^{-1}(\tanh|\kappa/2|) < \theta < \pi$.

Eqs. (1) and (2), with $\kappa \neq 0$, conserve the corresponding Hamiltonian, and the norm (frequently called *energy* in optics), $E \equiv \int_{-\infty}^{-\infty}(|u|^2 + |v|^2)\,dx$. For the exact soliton solution (3), $E_{\rm sol} \equiv 8\theta(1 - c^2)/(3 - c^2)$, while, for solution (4), $E = (8/3)[\theta - (\pi/2 - \sin^{-1}(\mathrm{sech}\,\kappa))\,\mathrm{sgn}\,\kappa]$ [12]. If $|\kappa|$ is small enough, the defect with $f(x) = \delta(x)$ creates an effective potential for a slowly moving soliton, $U(\xi) = -(8/3)\kappa(\sin^2\theta)/[\cosh(2\xi\sin\theta) + \cos\theta]$, where ξ is the coordinate of the soliton's center, and its effective mass is $M = (8/9)(7\sin\theta - 4\theta\cos\theta)$ [10]. In accordance with what was said above, this potential is attractive and repulsive for $\kappa > 0$ and $\kappa < 0$, respectively.

3. Capture of a free soliton

Numerical simulations of the collision of a free soliton with the dipole set (the attractive defect followed by the repulsive one) give rise to results summarized in Fig. 1(a), which displays the share of the soliton's energy trapped after the collision, the remaining energy being chiefly reflected (at small $|c|$) or transmitted (at larger $|c|$) in the form of small pulses, as shown in Fig. 1(b). We define the effective capture of the soliton as an outcome of the collision with the share of the trapped energy $\geqslant 65\%$. Fig. 1(a) demonstrates that the capture by the doublet, below the "65% capture limit" boundary, is possible for $|c| \leqslant 0.52$, which is a better result than the capture limit for a pair of repulsive defects, $|c| \leqslant 0.42$ [15] (which, in turn, was better than for single or paired attractive defects [12,15]). However, Fig. 1(b) clearly shows that the doublet traps the pulse in a strongly perturbed state; for this reason, the outcome of its subsequent collision with another free soliton is practically unpredictable, as it strongly depends on the intrinsic state of the trapped pulse at the moment of the new collision.

The triplet produces essentially better results. In fact, it may be considered as a generalization of the cavity formed by a pair of far separated repulsive defects, which was introduced in Ref. [15]; however, the small separation between them in the triplet, and the attractive defect inserted in the middle, help to capture more energy from the incident soliton, and shape the trapped energy into

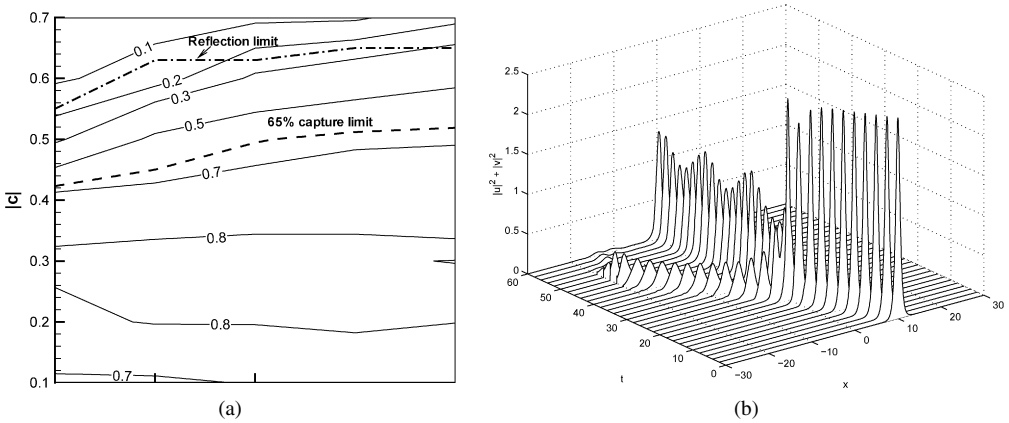

(a) (b)

Fig. 1. (a) Contour plots for the share of the energy of the free soliton with velocity c, trapped after its collision with the dipole (doublet) defect built as a set of the attractive and repulsive defects with strengths $\pm\kappa$. Above the "reflection limit" boundary, the soliton as a whole bounces back, due to the reflection from the repulsive defect. (b) An example of the collision for $c = -0.5c$ and $\theta = \pi/2$. In this figure and below, the defect is centered at $x = 0$, and the free soliton is always launched at $x = 10$.

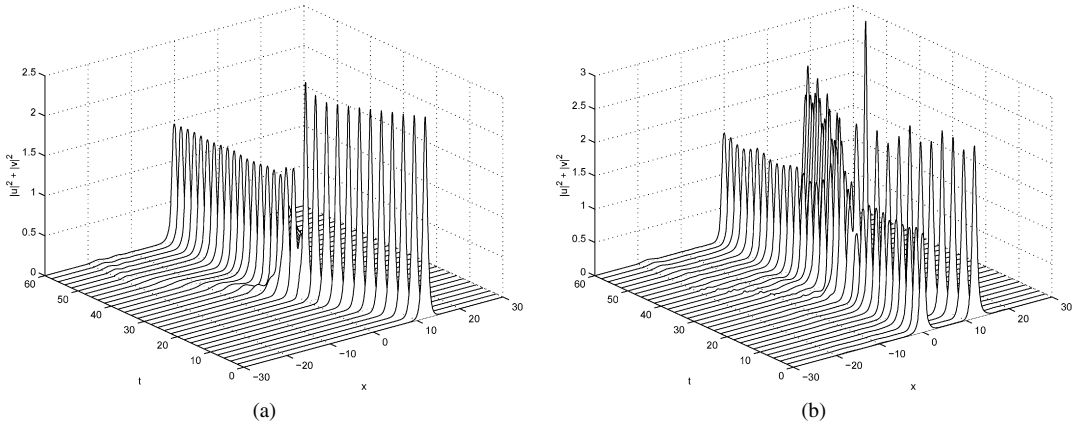

Fig. 2. Typical examples of collisions involving a triplet. (a) Capture of a free soliton by an empty triplet (the collision also generates a small reflected pulse, which is poorly seen behind the trapped soliton). (b) Bounce of a free moving soliton from the pinned one, which was generated by the collision shown in (a). In either case, the free soliton has amplitude $\theta = \pi/2$ and velocity $c = -0.5$. The triplet is a set of two repulsive defects, with $\kappa = -0.3$, and an attractive one between them, with $\kappa = +0.3$.

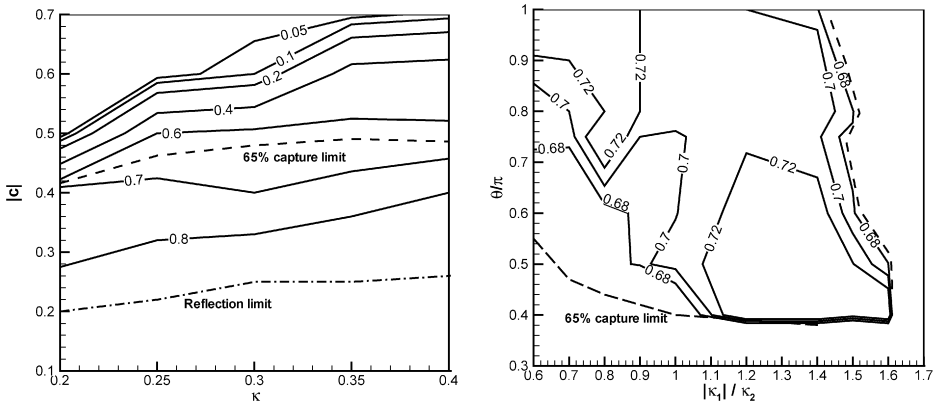

Fig. 3. (a) The same as in Fig. 1(a), but for the capture of a free moving soliton (with amplitude $\theta = \pi/2$) by the triplet formed by two repulsive defects with strengths $\kappa_1 \equiv -\kappa$, and an attractive one set between them, with strength $\kappa_2 \equiv \kappa$. Below the "reflection limit" boundary, the soliton as a whole bounces back (in fact, it is a sharp border between the capture and rebound). (b) The share of the captured energy versus amplitude θ of the free soliton, with velocity $c = -0.5$, and the ratio of the strengths of the repulsive and attractive defects, if their strengths are not equal.

a stationary pulse. A typical example of the capture by the triplet is displayed in Fig. 2(a). A noteworthy peculiarity of this figure, in comparison with the capture of solitons by single or paired defects [12,15], as well as by the dipole [see Fig. 1(b)], is that the trapped soliton immediately settles down into a stationary state, without any conspicuous intrinsic dynamics.

In a broad parameter range, the efficiency of the capture by the triplet is characterized by plots shown in Fig. 3. The capture limit is roughly the same as provided by the dipole, cf. Fig. 1(a), but the quality of the trapping is much better in the present case, as the trapped soliton is a stationary one, as demonstrated above. It is noteworthy that the capture efficiency is not sensitive to details of the triplet's structures, as seen in Fig. 3(b), which displays the share of the trapped energy versus the relative strength of the repulsive and attractive components of the triplet. The same figure demonstrates that "heavy" incident solitons, with $\theta > \pi/2$, which are intrinsically unstable [5,6], may also be used for the creation of stable trapped solitons, if the collision happens before the "heavy" soliton develops its instability. Another interesting feature of Fig. 3(b) is that there is a well-defined lower threshold for the amplitude of the free soliton, $\theta_{\min} \approx 0.4\pi$, which is necessary for the efficient capture.

4. Collisions between free and pinned solitons

Collisions between bound and free solitons were not studied before in the FBG model, even for a single attractive defect. Examined were collisions of two free solitons, against the backdrop of the single [13] or paired [15] defects. Sundry outcomes were found, including the capture of both solitons, which might merge into a single one [15] (collisions between free solitons in the uniform-FBG model were studied in detail in Ref. [19]).

As mentioned above, the outcome of the collision between a free soliton and one pinned by the dipole defect is very irregular, if the pinned soliton itself was generated by trapping an originally free one by the empty dipole, as, in that case, the pinned soliton

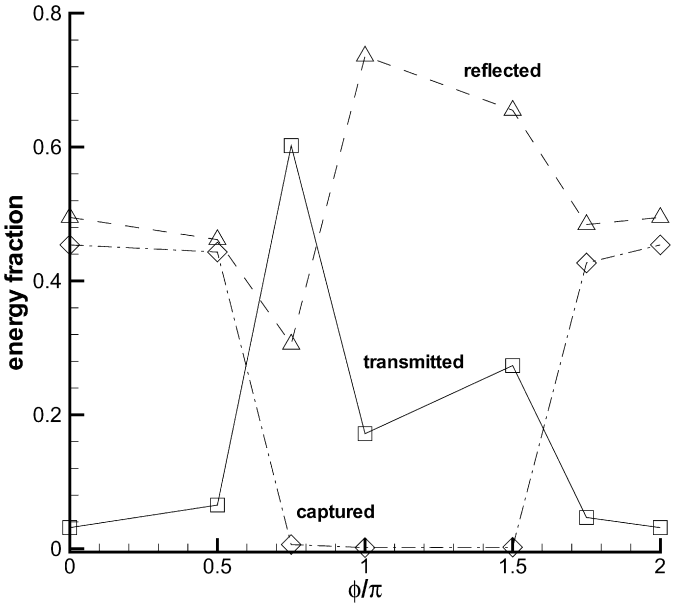

Fig. 4. Shares of the total energy of the colliding solitons (a free one and a soliton originally pinned by the triplet with $\kappa_2 = -\kappa_1 = 0.3$) which are eventually bound in the bouncing ("reflected") pulse and in ones which stay trapped ("captured") and move to the left, having been kicked out from the pinned state ("transmitted"). The initial amplitude of both solitons is $\theta = \pi/2$ (the bound soliton was generated by the capture of a free one with $\theta = \pi/2$). In (a), the shares are shown versus the velocity of the free soliton, for the collision with zero phase difference, $\phi = 0$; in (b), the same is shown versus ϕ, for $c = -0.5$. The three shares do not add up to 100%, as a small additional share is lost to radiation.

performs persistent intrinsic vibrations, and the outcome depends on the phase of the vibrations at the moment of the collision with the incident soliton. We have checked that essentially the same is observed if the first soliton was originally trapped by a single attractive defect. Obviously, this irregularity would impede the use of the collisions in applications.

On the contrary, the collision between the soliton originally captured by a triplet and a free soliton is completely predictable. While the incident soliton always bounces back, the pinned one either remains in the same state [see an example in Fig. 2(b)] or is kicked out in the forward direction, depending on the velocity of the free soliton, c, and phase shift ϕ between it and the pinned soliton at the collision moment. Small portions of the energy are spent to form additional weak pulses, as seen in Fig. 2(b). The dependence of the outcome of the collision on c and ϕ is displayed in Fig. 4. A sharp transition from the rebound without depinning to the release of the pinned soliton, in a narrow interval $0.55 < |c| < 0.6$, is observed in Fig. 4(a). It is quite natural that the increase of the momentum of the free soliton allows it to kick out the pinned one. Fig. 4(b) additionally shows that the collision effect (release of the pinned soliton) is stronger when the two solitons are phase-shifted by $\phi \simeq \pi$ (the free soliton, with the same momentum, kicks out the pinned one, unlike the situation at $\phi = 0$). The difference can be understood, as in-phase solitons attract each other, while out-of-phase ones interact with repulsion; therefore, in the former case the interaction force acts on the pinned soliton to the right (in the direction of the free soliton), hence it is less likely for it to be kicked out in the opposite direction, while the repulsion force, acting on it in the case of $\phi \simeq \pi$, makes the eventual depinning more plausible.

It is relevant to mention that the simulations did not reveal an outcome of the collision in the form of "recharge", i.e., replacement of the originally pinned soliton by the impinging one.

5. Conclusion

We have extended the recent analysis of the interaction of a free soliton in the FBG (fiber-Bragg-grating) model with a paired-defect set to a more complex (but still sufficiently simple) triplet structure, formed by two repulsive defects and an attractive one between them, with a relatively small separation between the defects. It has been demonstrated that the triplet is superior to other traps (including the doublet formed by attractive and repulsive defects) in achieving the aim of the creation of the "standing optical soliton": the triplet allows one to capture $2/3$ of the energy of a free soliton moving at half the light speed in the fiber. A moving intrinsically unstable ("too heavy") soliton can also be readily captured by the triplet, giving rise to the stationary pinned pulse. Another advantage offered by the triplet is that the trapped soliton quickly settles down to a stationary state, which makes the subsequent collision of the pinned soliton with a free one predictable: the impinging soliton always bounces back, while the pinned one remains in the bound state or is kicked out, depending on the velocity and relative phase of the collision. The triplet structure, whose inner scale is on the (sub)millimeter scale, can be readily fabricated in the FBG, and the predicted results may be relevant to the design of soliton-based optical memory and logic element, where solitons would serve as data bits.

References

[1] A.B. Aceves, S. Wabnitz, Phys. Lett. A 141 (1989) 37;
D.N. Christodoulides, R.I. Joseph, Phys. Rev. Lett. 62 (1989) 1746.
[2] C.M. de Sterke, J.E. Sipe, Prog. Opt. 33 (1994) 203.
[3] B.J. Eggleton, R.E. Slusher, C.M. de Sterke, P.A. Krug, J.E. Sipe, Phys. Rev. Lett. 76 (1996) 1627;
C.M. de Sterke, B.J. Eggleton, P.A. Krug, J. Lightwave Technol. 15 (1997) 1494.
[4] G. Van Simaeys, S. Coen, M. Haelterman, S. Trillo, Phys. Rev. Lett. 92 (2004) 223902.
[5] B.A. Malomed, R.S. Tasgal, Phys. Rev. E 49 (1994) 5787;
D.J. Kaup, T.I. Lakoba, J. Math. Phys. 37 (1996) 3442.
[6] I.V. Barashenkov, D.E. Pelinovsky, E.V. Zemlyanaya, Phys. Rev. Lett. 80 (1998) 5117;
A. De Rossi, C. Conti, S. Trillo, I.V. Barashenkov, D.E. Pelinovsky, E.V. Zemlyanaya, Phys. Rev. Lett. 81 (1998) 85.
[7] J. Marangos, Nature 397 (1999) 559;
K.T. McDonald, Am. J. Phys. 68 (2000) 293.
[8] J.E. Heebner, R.W. Boyd, Q.H. Park, Phys. Rev. E 65 (2002) 036619.
[9] J.T. Mok, C.M. de Sterke, I.C.M. Littler, B.J. Eggleton, Nature Phys. 2 (2006) 775.
[10] W.C.K. Mak, B.A. Malomed, P.L. Chu, J. Mod. Opt. 51 (2004) 2141.
[11] R.H. Goodman, R.E. Slusher, M.I. Weinstein, J. Opt. Soc. Am. B 19 (2002) 1635.
[12] W.C.K. Mak, B.A. Malomed, P.L. Chu, J. Opt. Soc. Am. B 20 (2003) 725.
[13] W.C.K. Mak, B.A. Malomed, P.L. Chu, Phys. Rev. E 67 (2003) 026608.
[14] C.M. de Sterke, E.N. Tsoy, J.E. Sipe, Opt. Lett. 27 (2002) 485.
[15] P.Y.P. Chen, B.A. Malomed, P.L. Chu, Phys. Rev. E 71 (2005) 066601.
[16] G. Kurizki, A.E. Kozhekin, T. Opatrny, B.A. Malomed, in: E. Wolf (Ed.), Progress in Optics, vol. 42, North-Holland, Amsterdam, 2001, pp. 93–146 (Chapter 2).
[17] I.V. Mel'nikov, B.I. Mantsyzov, J.S. Aitchison, Opt. Lett. 29 (2004) 289;
B.I. Mantsyzov, I.V. Mel'nikov, J.S. Aitchison, Phys. Rev. E 69 (2004) 055602;
B.I. Mantsyzov, I.V. Mel'nikov, J.S. Aitchison, IEEE J. Sel. Topics Quant. Electr. 10 (2004) 893.
[18] T. Iizuka, C.M. de Sterke, Phys. Rev. E 61 (2000) 4491.
[19] W.C.K. Mak, B.A. Malomed, P.L. Chu, Phys. Rev. E 68 (2003) 026609.